


RESEARCH

Open Access



# Transforming growth factor- $\beta$ 1 decreases erythropoietin production through repressing hypoxia-inducible factor 2 $\alpha$ in erythropoietin-producing cells

Hong-Mou Shih<sup>1,2</sup>, Szu-Yu Pan<sup>3,4,5</sup>, Chih-Jen Wu<sup>2,6,7</sup>, Yu-Hsiang Chou<sup>4,8</sup>, Chun-Yuan Chen<sup>9</sup>, Fan-Chi Chang<sup>4</sup>, Yi-Ting Chen<sup>3,4,8</sup>, Wen-Chih Chiang<sup>4</sup>, Hsing-Chen Tsai<sup>10,11</sup>, Yung-Ming Chen<sup>3</sup> and Shuei-Liong Lin<sup>1,3,4,12\*</sup> 

## Abstract

**Background:** Renal erythropoietin (EPO)-producing (REP) cells produce EPO through hypoxia-inducible factor (HIF) 2 $\alpha$ -activated gene transcription. Insufficient EPO production leads to anemia in patients with chronic kidney disease. Although recombinant EPO is effective to improve anemia, no reliable REP cell lines limit further progress of research and development of novel treatment.

**Methods:** We screened *Epo* mRNA expression in mouse fibroblast cell lines. Small interfering RNA specific for HIF1 $\alpha$  or HIF2 $\alpha$  was transfected to study *Epo* expression in C3H10T1/2 cells. The effect of transforming growth factor- $\beta$ 1 (TGF- $\beta$ 1) on HIF-EPO axis was studied in C3H10T1/2 cells and mice.

**Results:** Similar to mouse REP pericytes, C3H10T1/2 cells differentiated to  $\alpha$ -smooth muscle actin<sup>+</sup> myofibroblasts after exposure to TGF- $\beta$ 1. Specific HIF knockdown demonstrated the role of HIF2 $\alpha$  in hypoxia-induced *Epo* expression. Sustained TGF- $\beta$ 1 exposure increased neither DNA methyltransferase nor methylation of *Epas1* and *Epo* genes. However, TGF- $\beta$ 1 repressed HIF2 $\alpha$ -encoding *Epas1* promptly through activating activin receptor-like kinase-5 (ALK5), thereby decreasing *Epo* induction by hypoxia and prolyl hydroxylase domain inhibitor roxadustat. In mice with profibrotic injury induced by ureteral obstruction, upregulation of *Tgfb1* was accompanied with downregulation of *Epas1* and *Epo* in injured kidneys and myofibroblasts, which were reversed by ALK5 inhibitor SB431542.

**Conclusion:** C3H10T1/2 cells possessed the property of HIF2 $\alpha$ -dependent *Epo* expression in REP pericytes. TGF- $\beta$ 1 induced not only the transition to myofibroblasts but also a repressive effect on *Epas1-Epo* axis in C3H10T1/2 cells. The repressive effect of TGF- $\beta$ 1 on *Epas1-Epo* axis was confirmed in REP pericytes in vivo. Inhibition of TGF- $\beta$ 1-ALK5 signaling might provide a novel treatment to rescue EPO expression in REP pericytes of injured kidney.

**Keywords:** Erythropoietin, Hypoxia-inducible factor 2 $\alpha$ , Pericyte, Transforming growth factor- $\beta$ 1

## Background

Renal erythropoietin (EPO)-producing (REP) cells are interstitial platelet-derived growth factor receptor- $\beta$  (PDGFR $\beta$ )<sup>+</sup> pericytes, also known as perivascular fibroblasts [1–6]. In addition to produce EPO under conditions of anemia and hypoxia, pericytes produce growth factors to promote angiogenesis or microvascular

\*Correspondence: linsl@ntu.edu.tw

<sup>1</sup> Graduate Institute of Physiology, College of Medicine, National Taiwan University, No. 1, Jen-Ai Road Section 1, Taipei 100, Taiwan  
Full list of author information is available at the end of the article



© The Author(s) 2021. **Open Access** This article is licensed under a Creative Commons Attribution 4.0 International License, which permits use, sharing, adaptation, distribution and reproduction in any medium or format, as long as you give appropriate credit to the original author(s) and the source, provide a link to the Creative Commons licence, and indicate if changes were made. The images or other third party material in this article are included in the article's Creative Commons licence, unless indicated otherwise in a credit line to the material. If material is not included in the article's Creative Commons licence and your intended use is not permitted by statutory regulation or exceeds the permitted use, you will need to obtain permission directly from the copyright holder. To view a copy of this licence, visit <http://creativecommons.org/licenses/by/4.0/>. The Creative Commons Public Domain Dedication waiver (<http://creativecommons.org/publicdomain/zero/1.0/>) applies to the data made available in this article, unless otherwise stated in a credit line to the data.

stability [6–9]. In injured kidneys, however, pericytes are the precursors of myofibroblasts [3, 9–13]. Transforming growth factor (TGF)- $\beta$ 1, one of pro-fibrotic cytokines involved in the pathogenesis of renal fibrosis, can upregulate DNA methyltransferase (DNMT) which increases methylation of *Rasal1* and *Ybx2* genes in pericytes, thereby activating cell proliferation and  $\alpha$ -smooth muscle actin ( $\alpha$ -SMA) expression, respectively [9, 14]. Concomitant hypermethylation in the 5'-enhancer and promoter of *Epo* gene results in the repression of *Epo* in myofibroblasts and anemia in chronic kidney disease (CKD) [3]. In addition to *Epo* methylation, a variety of pathogenetic factors in CKD including inflammation, endoplasmic reticulum stress, oxidative stress and uremic toxin have been shown to reduce EPO production in the cell or animal models [1, 2, 15–20].

The kidney and liver produce about 90% and 10% of EPO in the adult, respectively, while the liver is the main source of EPO in the fetus [21–23]. Hence it is reasonable to use hepatic cell lines in the study of *Epo* gene regulation [16, 18, 24–26]. Decreased tissue oxygen tension appears to be the major factor triggering EPO production through hypoxia-inducible factor (HIF)-activated transcription [27, 28]. While the hypoxia response element (HRE)<sup>+</sup> 3'-enhancer of *Epo* gene is liver specific [26, 29], Storti et al. report a functional HIF2 $\alpha$ -dependent HRE in the distal 5'-enhancer located at kidney-inducible element (KIE) [30]. A number of attempts to generate REP cell lines have been reported [31–33]. In fibroblast-like 4E cells isolated from the adult mouse kidney, the subset of CD73<sup>+</sup> cells are capable of expressing *Epo* under hypoxia [31]. REP cells isolated from severe neonatal anemic mice (*Epo*<sup>GFP/A3'E</sup>) provide the evidence of HIF in the regulation of renal EPO production [32]. Renal CD133<sup>+</sup>/CD73<sup>+</sup> mesenchymal progenitor cells, isolated from the inner medulla of human kidneys, produce EPO under hypoxia through HIF2 $\alpha$  [33]. We also provide evidence that primary Col1a1-GFP<sup>+</sup> pericytes isolated from *Col1a1-GFP*<sup>Tg</sup> mice are capable of producing EPO under hypoxia [3]. However, Col1a1-GFP<sup>+</sup> pericytes differentiate to myofibroblasts after passages and decrease *Epo* expression due to hypermethylation in the promoter and 5'-distal enhancer of *Epo* gene [3]. Hence, no success has been achieved in establishing reliable REP cell lines with capability of regulated EPO expression until recently [19, 20]. Fibroblastoid atypical interstitial kidney (FAIK) cells are obtained by isolation of primary REP cells from *Epo-CreERT2*<sup>Tg</sup>;*Rosa26*<sup>fsttdTomato/+</sup> mice and then immortalized with SV40 large T antigen [19]. FAIK cells maintain hypoxia-induced EPO expression, even at rather low levels, for at least 30 passages. Interestingly, demethylating agent 5-azacytidine can enhance both basal and hypoxia-induced EPO expression in FAIK cells, confirming the

repressive effect of methylation induced by SV40 large T antigen [3, 19]. A second cell line, REP cell-derived immortalized and cultivable cell line (Replic cells), is obtained by isolation of primary REP cells from a gene-modified mouse line (ISAM-REC) and then immortalized by lentiviral transduction of human *HRAS* gene [20]. Interestingly, Replic cells exhibit myofibroblastic phenotypes due to autonomous TGF- $\beta$ 1 signaling and lose the EPO production [1–3, 20]. Hypermethylation of *Epo* gene in Replic cells is also demonstrated, a finding in line with the possible consequence of overexpressing human RAS [19, 20, 34, 35].

Renznikoff et al. have reported the establishment of C3H10T1/2 (hereafter referred to as 10T1/2) cell line from C3H mouse embryo [36]. Previous study has shown that 10T1/2 cells can be differentiated to pericytes to support the formation of capillary-like structure in three-dimensional co-culture with endothelial cells [37]. The findings that 10T1/2 cells can stabilize microvasculature and transit to myofibroblasts are similar to that we demonstrate in the primary culture of kidney pericytes [3, 8, 9, 38, 39]. We therefore studied the properties of EPO expression in 10T1/2 cells and used murine model to prove the findings from cell line study.

## Materials and methods

### Cell culture

Mouse fibroblast cell lines, 10T1/2 (ATCC CCL-226) and NIH/3T3 (hereafter referred to as 3T3, ATCC CRL-1658) were maintained in DMEM/F12 (Invitrogen, Carlsbad, CA) supplemented with 10% fetal bovine serum (FBS, Hyclone, Marlborough, MA). In hypoxia experiments, cells were placed in an incubator with 21% O<sub>2</sub> or in a hypoxia chamber (INVIVO2 200, Ruskinn Technology Ltd., Bridgend, UK) with 0.5% O<sub>2</sub> for indicated duration. Cellular RNA was harvested by adding the TRIzol reagent (Invitrogen) or RNeasy mini kit (Qiagen, Valencia, CA) immediately after cells were taken out of the incubator and the supernatant was removed for storage. In roxadustat (MedChemExpress LLC, Monmouth Junction, NJ) experiments, cells were washed with 1  $\times$  PBS and renewed culture medium with or without roxadustat (50  $\mu$ M). Cellular RNA was harvested at indicated time points. In TGF- $\beta$ 1 stimulation experiments, cells were washed with 1  $\times$  PBS and renewed culture medium with or without 5 ng/mL TGF- $\beta$ 1 (R&D Systems, Minneapolis, MN) in the presence of 5  $\mu$ g/mL TGF- $\beta$  receptor-1 (TGF- $\beta$ R1) activin receptor-like kinase-5 (ALK5) inhibitor (ALK5i) SB431542 (Tocris Bioscience, Bristol, UK) or vehicle. Cellular RNA were harvested at indicated time points.

### Quantitative polymerase chain reaction (PCR)

The purity of RNA sample was determined based on the ratio of A260 to A280. cDNA was synthesized using the iScript cDNA Synthesis Kit (Bio-Rad, Hercules, CA). Quantitative PCR was performed using methods described previously [40]. The specific primer pairs used for PCR were listed in Additional file 1: Table S1.

### Western blot analysis

Whole cell lysates were prepared using radioimmunoprecipitation assay (RIPA) buffer supplemented with Protease Inhibitor Cocktail (Roche, Mannheim, Germany) and Phosphatase Inhibitor Cocktail (Roche). For HIF protein, cells were harvested by RIPA buffer in hypoxia chamber. Forty micrograms of cell lysate were heated at 95 °C for 8 min, applied to sodium dodecyl sulphate-polyacrylamide (7.5%) gel electrophoresis. A prestained marker was also electrophoresed as a molecular weight marker. The proteins were then transferred onto a polyvinylidene fluoride membrane (Millipore, Burlington, MA) using a transblot chamber with Tris buffer. Western blots were incubated at 4 °C overnight with primary antibodies. The next morning, membranes were washed with TBS/Tween-20 at room temperature 3 times for 5 min each and incubated with horseradish peroxidase (HRP)-conjugated secondary antibodies at room temperature for two hours. After washing, the membranes were incubated with Immobilon Classico Western HRP substrate (Millipore) according to the manufacturer's instructions. The following primary antibodies were used to detect protein: HIF1 $\alpha$  (PAB12138; Abnova, Taipei, Taiwan), HIF2 $\alpha$  (C150132; LSBio, Seattle, WA), p-Smad2/3 (SC-11769-R; Santa Cruz Biotechnology, Santa Cruz, CA), total Smad2/3 (3102; Cell Signaling Technology, Danvers, MA),  $\alpha$ -tubulin (ab176560; Abcam, Cambridge, UK),  $\beta$ -actin (4967; Cell Signaling), GAPDH (Ab9485; Abcam) and proliferating cell nuclear antigen (PCNA, RB-9055; Thermo Scientific, Fremont, CA).

### Transfection

Small interfering RNA (siRNA) experiments were carried out with Dharmafect transfection reagent (Dharmacon, Lafayette, CO), according to the manufacturer's protocol. siRNA oligos were obtained as SMART-pools from Dharmacon. Silencing of *Hif1a* and/or *Epas1* were performed by transfection of ON-TARGET plus Mouse *Hif1a* and *Epas1* siRNA (5 nM). As control, non-targeting siRNA was used.

### Detection of EPO in culture media

Cell culture supernatant were stored in a - 80 °C freezer after collection, transferred into a - 20 °C freezer

12–16 h prior to analysis and thawed on ice before analysis. The analysis was performed according to the protocol of provided in the Mouse Erythropoietin Quantikine ELISA Kit (R&D Systems).

### Chromatin immunoprecipitation (ChIP)

ChIP was performed using a ChIP kit (Magna ChIP A/G, Millipore) according to the manufacturer's protocol. Protein-DNA complexes were cross-linked by incubating 10T1/2 cells with 1% formaldehyde for 10 min. Glycine was added for 5 min to quench formaldehyde. Nuclear extraction using cell lysis buffer and nuclear lysis buffer supplemented with Protease Inhibitor Cocktail and MG-132 (Millipore) were sonicated to shear the chromatin to an average length of about 100~500 bp. Then the lysates were centrifuged for 10 min and supernatant was collected. Anti-HIF1 $\alpha$  (NB100-449), anti-HIF2 $\alpha$  (NB100-122, Novus Biologicals, Centennial, CO) antibody, or Rabbit IgG (SC-3888, Santa Cruz Biotechnology) were added with magnetic beads in the supernatant and incubated overnight at 4 °C with rotation. The magnetic bead-antibody/chromatin complex was washed and separated by magnetic separator. DNA was purified and amplified by PCR with primers listed in Additional file 1: Table S2. The PCR products were analyzed by electrophoresis and shown as a virtual gel. Quantitative PCR was performed using methods described previously [40]. The result was shown after normalization by the expression using input DNA as the PCR template.

### Methylation specific PCR (MSP)

Genomic DNA was prepared using DNeasy Blood & Tissue Kits (Qiagen). Sodium bisulfite conversion of genomic DNA was performed using the EZ DNA Methylation Kit according to the manufacturer's protocol (ZYMO Research, Irvine, CA). PCR using bisulfite-converted genomic DNA was amplified with methylation-specific or unmethylation-specific primer pairs listed in Additional file 1: Table S3. Unmethylated and methylated controls were from mouse sperm genomic DNA and Methylated Mouse Genomic DNA Standard (ZYMO Research), respectively. The PCR products were analyzed by electrophoresis. The electrophoresis result was shown as a virtual gel. The percentage of methylation of *Epo* 5'-flanking region or *Epas1* 5'-flanking region for the indicated cells was determined by densitometric analysis of MSP products (methylated products divided by the sum of methylated and unmethylated products).

### Animals

C57BL/6 wild type (WT) mice were obtained from The Jackson Laboratory (Bar Harbor, ME). *Col1a1-GFP<sup>Tg</sup>* mice were generated in the C57BL/6 background as

previously described [10]. Adult (8–10 weeks) mice were used for all experiments. Kidney samples for mRNA analyses were obtained. In mouse models of kidney fibrosis experiments, unilateral ureteral obstruction (UUO) was performed in adult mice as previously described [40]. Briefly, the left ureter was ligated twice using 4–0 nylon surgical sutures at the level of the lower pole of kidney. For experiments of blocking TGF- $\beta$ 1 signaling in vivo, mice were injected intraperitoneally with the ALK5i SB431542 (5 mg/kg per day) (Tocris Bioscience) 2 h before surgery and then as scheduled until euthanasia at day 4. Col1a1-GFP<sup>+</sup> pericytes and myofibroblasts were purified from kidneys before and after UUO surgery respectively using a method described previously [3]. Briefly, the kidney was decapsulated, diced and then incubated at 37°C for 40 min with collagenase (50 mg/ $\mu$ l, Roche) and dispase (0.3 U/ $\mu$ l, Roche) in Hank's Balanced Salt Solution (Sigma-Aldrich, St. Louis, MO). After centrifugation, cells were resuspended in 3 mL of PBS/1% BSA and filtered (40  $\mu$ m). Col1a1-GFP<sup>+</sup> pericytes and myofibroblasts were isolated from the single-cell preparation by sorting GFP<sup>+</sup>F4/80-APC<sup>-</sup>CD31-APC<sup>-</sup>CD324-APC<sup>-</sup> cells using a FACSaria cell sorter (BD Biosciences, San Jose, CA).

#### Statistics

Data were expressed as the mean  $\pm$  standard error of the mean (SEM). One-way ANOVA with post hoc Tukey's correction was used for the comparison between each group. Two-tailed Student's t-test was used to compare two different groups. A P value < 0.05 was considered significant. Statistical analyses were carried out using the GraphPad Prism software (GraphPad Software, La Jolla, CA).

## Results

### 10T1/2 cells exhibited a fibroblastic phenotype

10T1/2 cells displayed fibroblastic morphology on cell culture dishes (Fig. 1a). To study the cell type-specific expression, we performed quantitative PCR and compared the gene expression to that of 3T3 fibroblasts (Fig. 1b–e). Kidney was used as a control and its gene expression reflected the composition of multiple cell types. Similar to 3T3 fibroblasts, 10T1/2 cells did not express *Cdh1*, *Vegfr2*, *Nphs1* and *Nphs2* which encoded E-cadherin, vascular endothelial growth factor receptor 2, nephrin and podocin, respectively (Fig. 1b–d). Both 3T3 and 10T1/2 cells expressed *Pdgfra* and *Pdgfrb* which encoded PDGFR $\alpha$  and PDGFR $\beta$ , respectively (Fig. 1e). Compared to 3T3 cells, 10T1/2 cells notably expressed higher levels of *Acta2*, *Ng2* and *Nt5e* which encoded  $\alpha$ -SMA, neuron-gial antigen 2 and ecto-5'-nucleotidase, respectively (Fig. 1e). We also studied the marker for

cell proliferation and demonstrated that 10T1/2 cells expressed lower level of *Ki67* (Fig. 1f). Nevertheless, both 3T3 and 10T1/2 cells could grow to confluence on cell culture dishes.

### 10T1/2 cells produced EPO in hypoxia and under PHD inhibition

Multiple genes are regulated by hypoxia in order to induce adaptive response. In addition to *Epo*, *Hif1a* and *Epas1*, we studied the common hypoxia response genes including *Vegfa*, *Egln1*, *Egln3* and *Slc2a1*. Compared to those in the chambers with 21% O<sub>2</sub>, 10T1/2 cells in the chambers with 0.5% O<sub>2</sub> substantially increased the expression of *Epo*, *Vegfa*, *Egln1* and *Egln3* which encoded EPO, vascular endothelial growth factor-A (VEGF-A), prolyl hydroxylase domain (PHD) 2 and PHD3, respectively (Fig. 2a). The expression of *Hif1a* which encoded HIF1 $\alpha$  was not changed by hypoxia, but in contrast, the expression of *Epas1* which encoded HIF2 $\alpha$  was drastically decreased (Fig. 2a). Interestingly, *Epo* and *Epas1* were not detected in 3T3 cells (Fig. 2a). In contrast to the upregulation of *Slc2a1* which encoded solute carrier family 2 member 1 in 3T3 cells by hypoxia, the expression of *Slc2a1* in 10T1/2 cells was not changed by hypoxia (Fig. 2a). It was worth noting that *Epo* expression in 10T1/2 cells was extremely low when compared to that of REP pericytes in normal kidneys (Fig. 2a). Increased EPO was demonstrated in the supernatant of 10T1/2 cells in hypoxia (Fig. 2b). In addition to hypoxia, the PHD inhibitor (PHDi) roxadustat also increased *Epo* expression in 10T1/2 cells substantially (Fig. 2c).

### Hypoxia induced *Epo* through HIF2 $\alpha$ in 10T1/2 cells

Both HIF1 $\alpha$  and HIF2 $\alpha$  increased expression in 10T1/2 cells after 3-h exposure to hypoxia (Fig. 3a) or PHDi (Additional file 2: Fig. S1). We transfected siRNA for *Hif1a* (siHif1a) or *Epas1* (siEpas1) to study the role of HIF1 $\alpha$  and HIF2 $\alpha$  in *Epo* induction by hypoxia. SiHif1a and siEpas1 specifically decreased the expression of *Hif1a*/HIF1 $\alpha$  and *Epas1*/HIF2 $\alpha$  in hypoxia, respectively (Fig. 3b–e). SiHif1a decreased the induction of *Epo*, *Egln1*, *Vegfa* and *Slc2a1* in hypoxia, whereas siEpas1 decreased the induction of *Epo*, *Egln3* and *Vegfa* in hypoxia (Fig. 3e, Additional file 2: Fig. S2). Notably, the inhibitory effect of HIF2 $\alpha$  knockdown on *Epo* induction was substantially higher and not augmented by concomitant HIF1 $\alpha$  knockdown (Fig. 3e), but both HIF1 $\alpha$  knockdown and HIF2 $\alpha$  knockdown contributed to the inhibitory effect on *Vegfa* induction (Additional file 2: Fig. S2). Using antibodies specific for HIF1 $\alpha$  or HIF2 $\alpha$  to precipitate chromatin, we demonstrated that hypoxia induced the most apparent binding of HIF2 $\alpha$  to distal 5'-enhancer of *Epo* gene (Fig. 4a). Quantitative



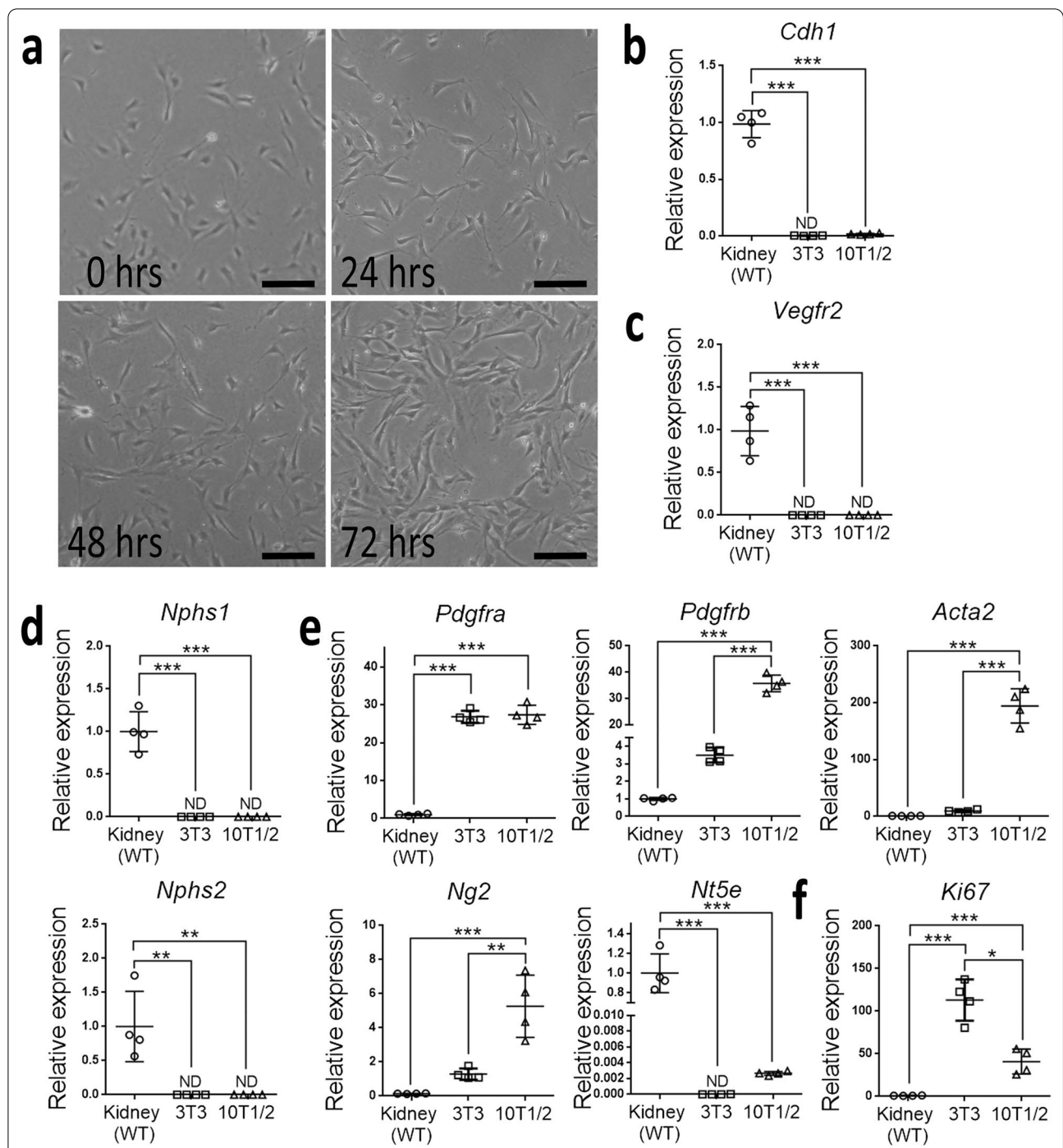
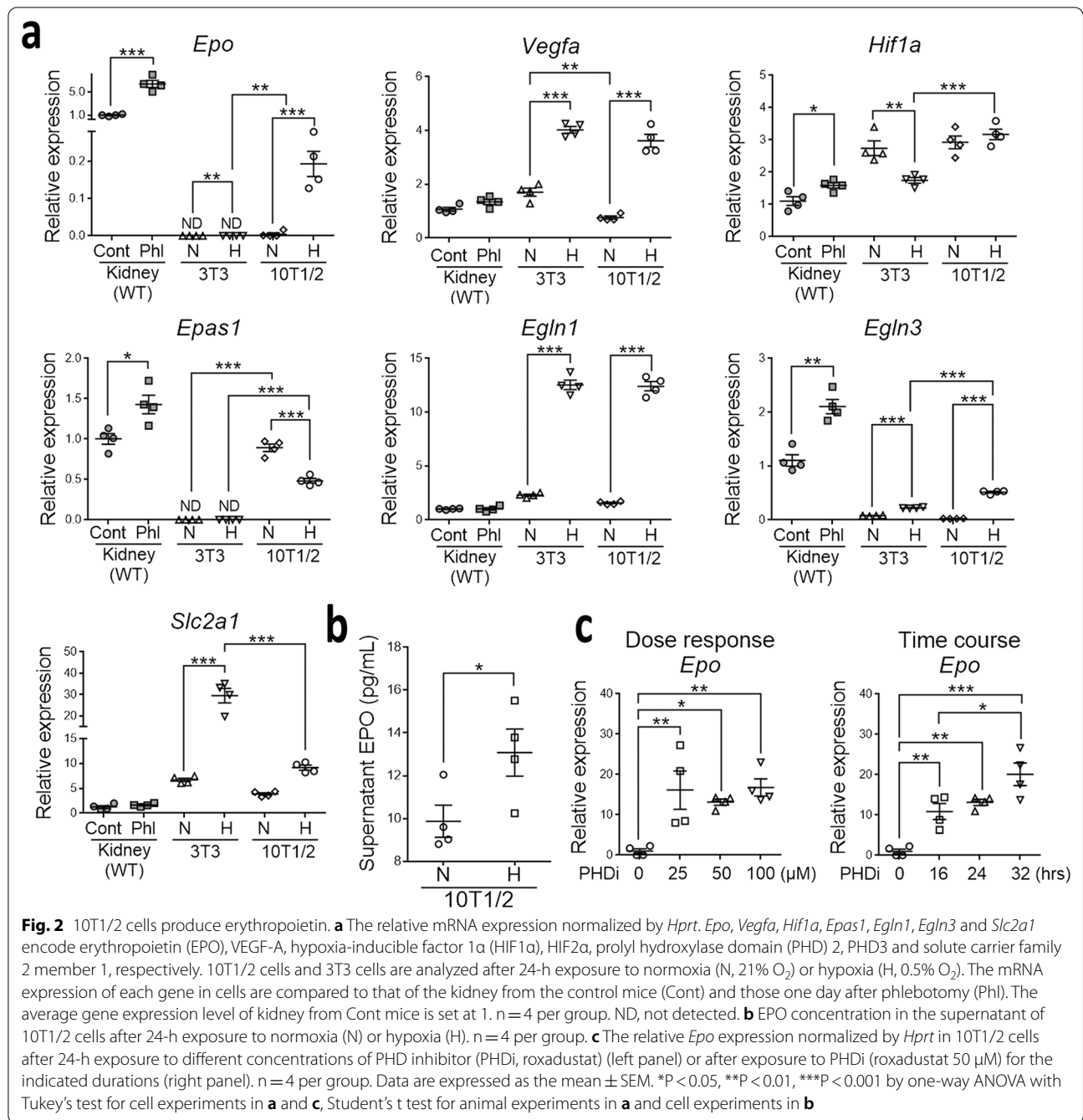
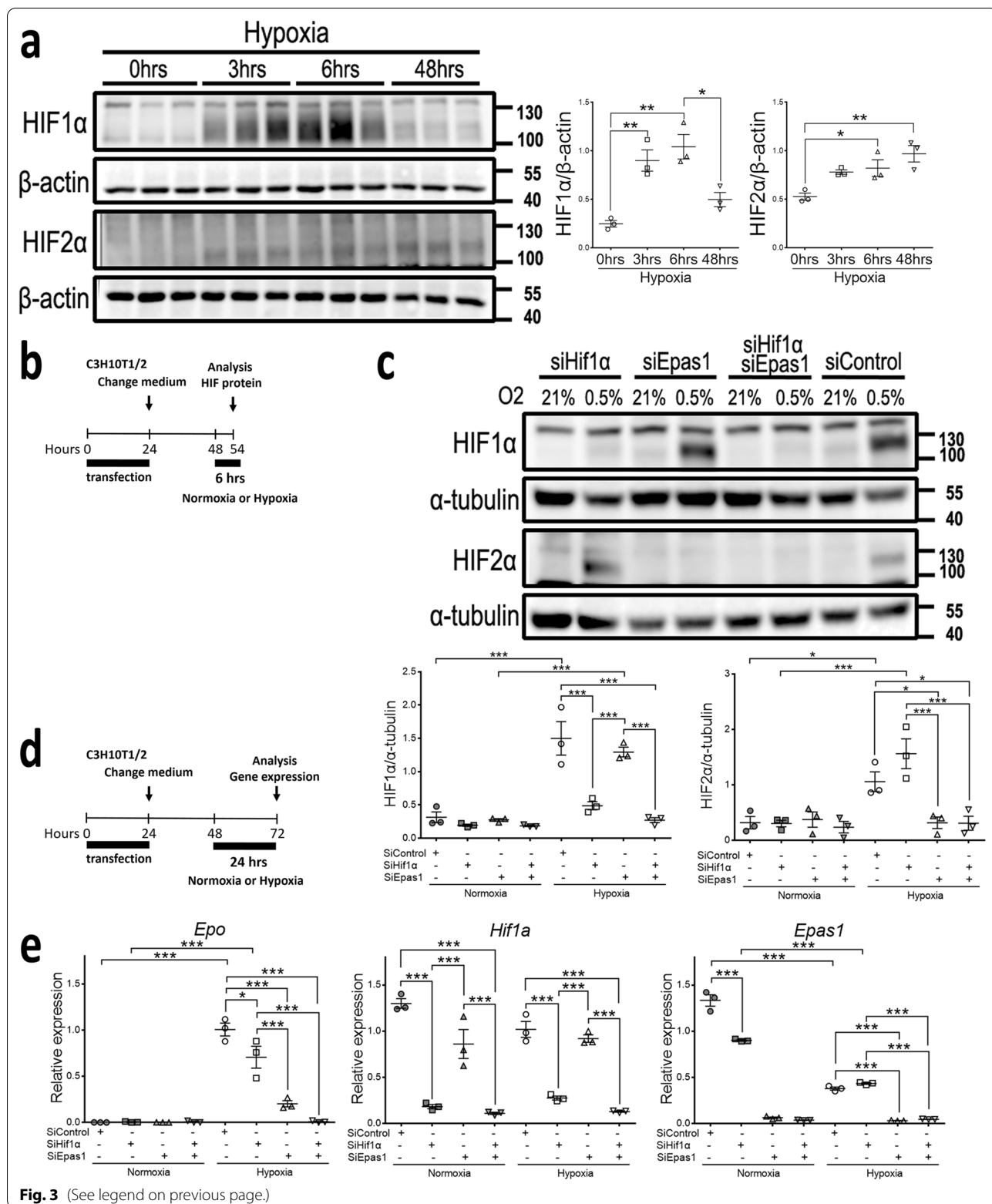


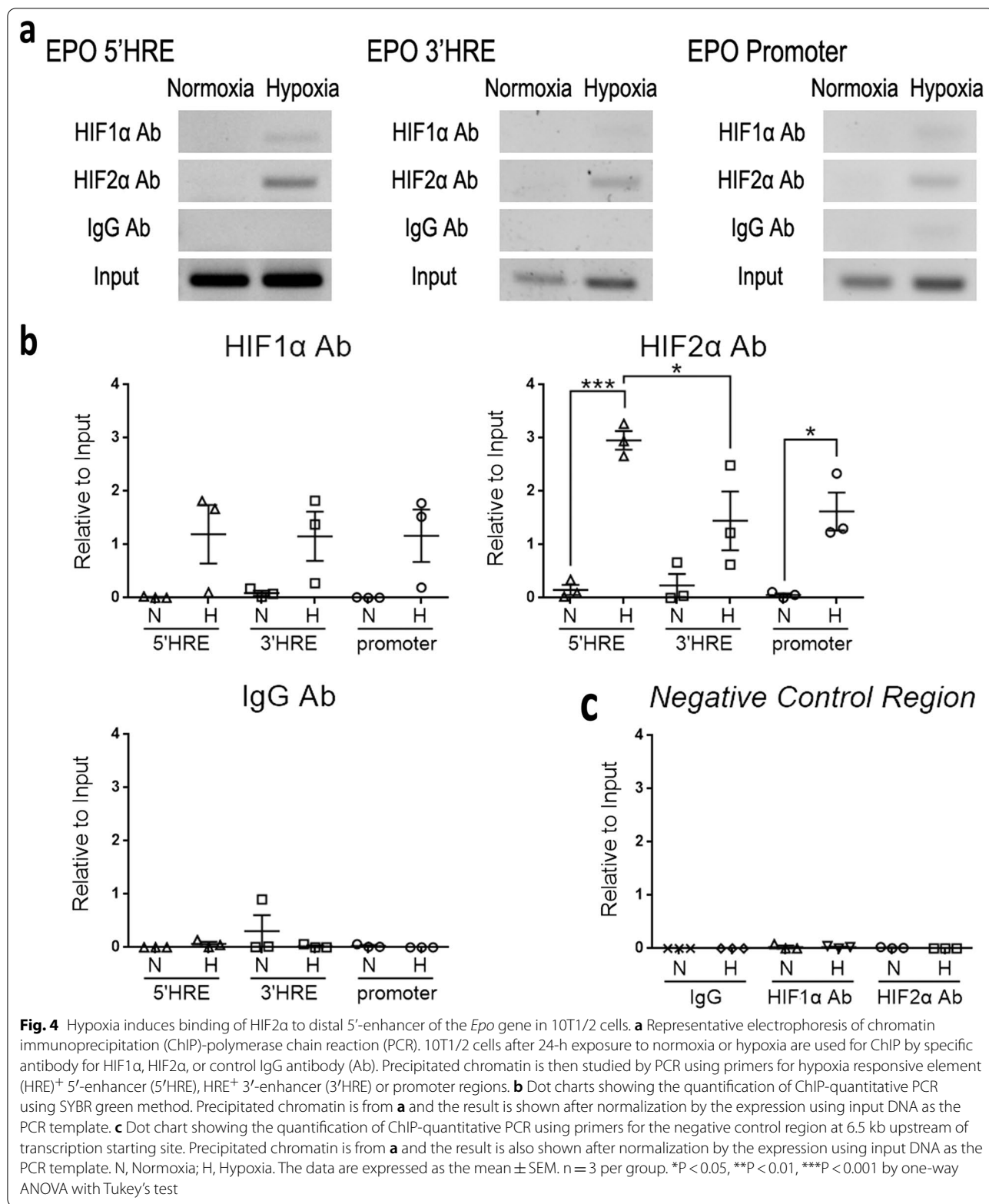
**Fig. 1** C3H10T1/2 cells exhibit a fibroblastic phenotype. **a** Bright-field images of C3H10T1/2 (referred to as 10T1/2) cells on cell culture dishes at the indicated time points after culture. Original magnification,  $\times 400$ . Scale bar: 200  $\mu\text{m}$ . **b–f** The relative mRNA expression normalized by *Hprt*. *Cdh1* encodes the epithelial cell marker E-cadherin; *Vegfr2* encodes the endothelial cell marker vascular endothelial growth factor (VEGF) receptor 2; *Nphs1* and *Nphs2* encode the podocyte markers nephrin and podocin, respectively; *Pdgfra*, *Pdgfrb*, *Acta2*, *Ng2* and *Nt5e* encode the fibroblast markers, platelet-derived growth factor receptor (PDGFR)  $\alpha$ , PDGFR $\beta$ ,  $\alpha$ -smooth muscle actin ( $\alpha$ -SMA), neuron-gial antigen 2 and ecto-5'-nucleotidase, respectively; *Ki67* encodes the marker for the assessment of cellular proliferative activity, Ki67 antigen; *Hprt* encodes hypoxanthine–guanine phosphoribosyl transferase and serves as the internal control. The gene expression of 10T1/2 cells is compared with those of 3T3 cells and the kidney from C57BL/6 wild type (WT) mice. The average expression of the kidney is set at 1. ND, not detected. The data are expressed as the mean  $\pm$  standard error of the mean (SEM).  $n = 4$  per group. \* $P < 0.05$ , \*\* $P < 0.01$ , \*\*\* $P < 0.001$  by one-way ANOVA with Tukey's test



(See figure on next page.)

**Fig. 3** Hypoxia induces *Epo* through HIF2a in 10T1/2 cells. **a** Representative Western blot analysis for the expression of HIF1a and HIF2a in hypoxia chamber (0.5% O<sub>2</sub>) for the indicated duration. Right panels showing the expression of HIF1a and HIF2a normalized by β-actin. n = 3 per group. **b** Schema illustrating the siRNA transfection specific for *Hif1a* (siHif1a), *Epas1* (siEpas1) or control (siControl) and culture medium refresh. HIFs are analyzed after 6-h exposure to normoxia or hypoxia. **c** Upper panel showing the representative Western blot analysis for the expression of HIF1a and HIF2a after siRNA transfection and exposure to normoxia/hypoxia as indicated. Lower panels showing the expression of HIF1a and HIF2a normalized by α-tubulin. n = 3 per group. **d** Schema illustrating the siRNA transfection and culture medium refresh. Gene expression is analyzed after 24-h exposure to normoxia or hypoxia. **e** The relative mRNA expression of *Epo*, *Hif1a* and *Epas1* normalized by *Hprt*. n = 3 per group. Data are expressed as the mean ± SEM. \*P < 0.05, \*\*P < 0.01, \*\*\*P < 0.001 by one-way ANOVA with Tukey's test in **a**, **c** and **e**







PCR of the precipitated chromatin confirmed that hypoxia induced significant binding of HIF2 $\alpha$  to distal 5'-enhancer and promoter, but not 3'-enhancer (Fig. 4b). In contrast, hypoxia did not induce significant binding of HIF1 $\alpha$  to distal 5'-enhancer, promoter and 3'-enhancer (Fig. 4b). Region at 6.5 kb upstream of the *Epo* transcription starting site served as the negative control (Fig. 4c). These data demonstrated HIF2 $\alpha$  as the major transcriptional factor for hypoxia-induced *Epo* expression in 10T1/2 cells.

**Low methylation in 5'-flanking regions of *Epo* and *Epas1* genes in 10T1/2 cells**

Since 10T1/2 cells, not 3T3 cells, expressed *Epo* and *Epas1*, we were curious about their epigenetic difference in *Epo* and *Epas1* genes. We focused on the methylation of *Epo* and *Epas1* gene in this study. Using MSP, we demonstrated hypermethylation in 5'-flanking regions of *Epo* and *Epas1* genes in 3T3 cells at the level comparable to the methylated control (Fig. 5a, b). The levels of methylation in *Epo* and *Epas1* genes were substantially lower in 10T1/2 cells (Fig. 5a, b). In addition to undetectable

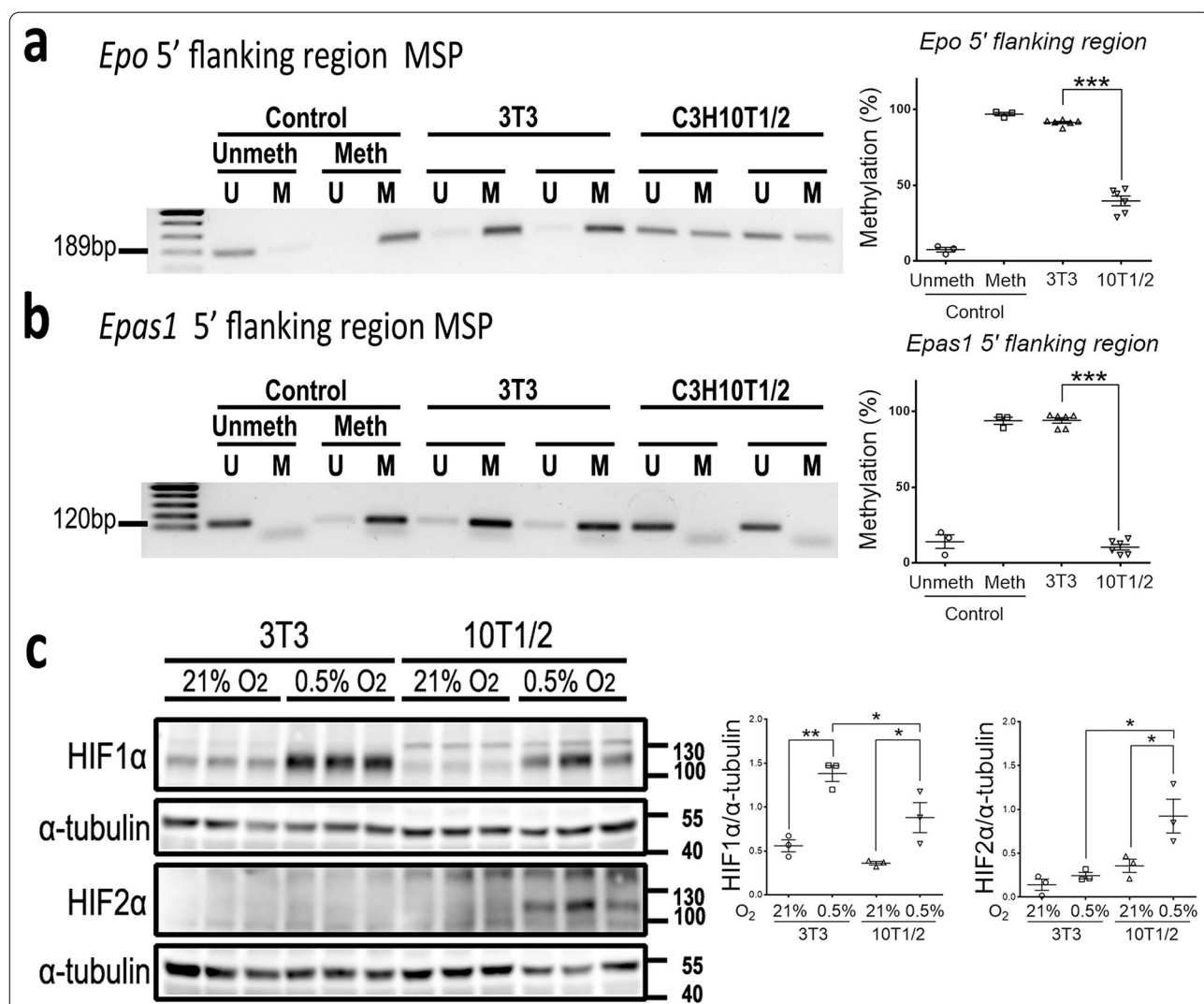


**Fig. 5** Low methylation in 5'-flanking regions of *Epo* and *Epas1* genes in 10T1/2 cells. **a, b** Representative electrophoresis of methylation specific PCR (MSP) using primers for the unmethylated (U) and methylated (M) 5'-flanking regions of *Epo* gene and *Epas1* gene from 3 independent experiments. Right panels showing the percentage of 5'-flanking region methylation determined by the densitometric analysis of the MSP products. The methylation levels in 3T3 cells are used for comparison. Data are expressed as the mean  $\pm$  SEM. \*\*\*P < 0.001 by Student's t test. Meth, methylated; Unmeth, unmethylated controls. **c** Representative Western blot analysis for HIF1 $\alpha$ , HIF2 $\alpha$  and  $\alpha$ -tubulin in 10T1/2 and 3T3 cells after 6-h exposure to normoxia (21% O<sub>2</sub>) or hypoxia (0.5% O<sub>2</sub>). Right panels showing the expression of HIF1 $\alpha$  and HIF2 $\alpha$  which is normalized by  $\alpha$ -tubulin. n = 3 per group. Data are expressed as the mean  $\pm$  SEM. \*P < 0.05, \*\*P < 0.01 by one-way ANOVA with Tukey's test

*Epas1* mRNA, we further confirmed that HIF2 $\alpha$  protein could not be induced by hypoxia in 3T3 cells (Fig. 5c).

#### 10T1/2 cells exhibited higher level of TGF- $\beta$ 1-ALK5 signaling and pro-fibrotic phenotype

Since REP pericytes possess cellular plasticity for myofibroblast transition when the kidney is damaged and TGF- $\beta$ 1 signaling is activated [2, 3], we studied the TGF- $\beta$ 1 signaling in both 10T1/2 and 3T3 cells. Compared to 3T3 cells, 10T1/2 cells expressed higher levels of *Tgfb1* and *Tgfb2* which encoded TGF- $\beta$ R1 and TGF- $\beta$ R2, respectively (Additional file 2: Fig. S3a). Western blot analysis revealed higher levels of phosphorylated SMAD2/3 in 10T1/2 (Additional file 2: Fig. S3b), a possible mechanism responsible for the higher expression of *Acta2*, *, *Col1a1* and *Col3a1* which encoded  $\alpha$ -SMA, fibronectin, type 1 collagen ( $\alpha$ 1 chain) and type 3 collagen ( $\alpha$ 1 chain), respectively (Fig. 1e, Additional file 2: Fig. S3c). However, the expression of *Serpine1*, which encoded plasminogen activator inhibitor-1, was lower in 10T1/2 cells (Additional file 2: Fig. S3c). The expression levels of *Acta2*, *Fn1*, *Col1a1* and *Serpine1* were extremely high in both 3T3 cells and 10T1/2 cells (Additional file 2: Fig. S3c), possibly because 3T3 cells and 10T1/2 cells are fibroblasts and kidneys are composed of heterogenous cell types.*

Activation of downstream signaling in 10T1/2 cells was demonstrated by the prompt phosphorylation of Smad2/3 after exposure to TGF- $\beta$ 1, which could be inhibited by ALK5i SB431542 (Fig. 6a, b). TGF- $\beta$ 1-stimulated 10T1/2 cells became more pro-fibrotic through upregulation of *Acta2*, *Col1a1*, *Fn1*, *Tgfb1* and *Serpine1*, which was also reversed by ALK5i SB431542 (Fig. 6a, c). UO injury increased expression of pro-fibrotic genes in the kidneys (Fig. 6c). Although the expression levels of these pro-fibrotic genes in kidneys were extremely lower than those in 10T1/2 cells, the heterogenous cell components in kidneys made the comparison between kidneys and 10T1/2 cells unsuitable.

#### TGF- $\beta$ 1 repressed *Epas1-Epo* axis through ALK5 in 10T1/2 cells

In addition to induce the pro-fibrotic phenotype of 10T1/2 cells (Fig. 6c), TGF- $\beta$ 1 inhibited *Epas1* expression substantially, an effect noted as early as after 6-h exposure to TGF- $\beta$ 1 (Fig. 7a). Therefore, we studied the effect of TGF- $\beta$ 1 on HIF expression in 10T1/2 cells (Fig. 7b, c, Additional file 2: Fig. S4a, b). TGF- $\beta$ 1 inhibited the expression of HIF2 $\alpha$ , but not HIF1 $\alpha$  induced by hypoxia or PHDi (Fig. 7c, Additional file 2: Fig. S4b). In the presence of ALK5i SB431542, the inhibitory effect of TGF- $\beta$ 1 on HIF2 $\alpha$  expression induced by hypoxia or PHDi was abolished (Fig. 7d, e, Additional file 2: Fig. S4c, d). In addition, the inhibitory effect of TGF- $\beta$ 1 on *Epas1*

expression was also ALK5 dependent (Fig. 7f, g). Meanwhile, hypoxia-induced nuclear accumulation of HIF2 $\alpha$  was inhibited by TGF- $\beta$ 1 through ALK5 (Additional file 2: Fig. S5). In consequence, the induction of *Epo* in hypoxia was inhibited by TGF- $\beta$ 1 through ALK5 (Fig. 7f, g). In contrast, TGF- $\beta$ 1 increased the expression of *Hif1a* in normoxia and hypoxia through ALK5, but did not affect the expression of HIF1 $\alpha$  (Fig. 7c, e, g). Moreover, TGF- $\beta$ 1 further increased the expression of *Egln1*, *Slc2a1* and *Vegfa* in hypoxia through ALK5 (Additional file 2: Fig. S6).

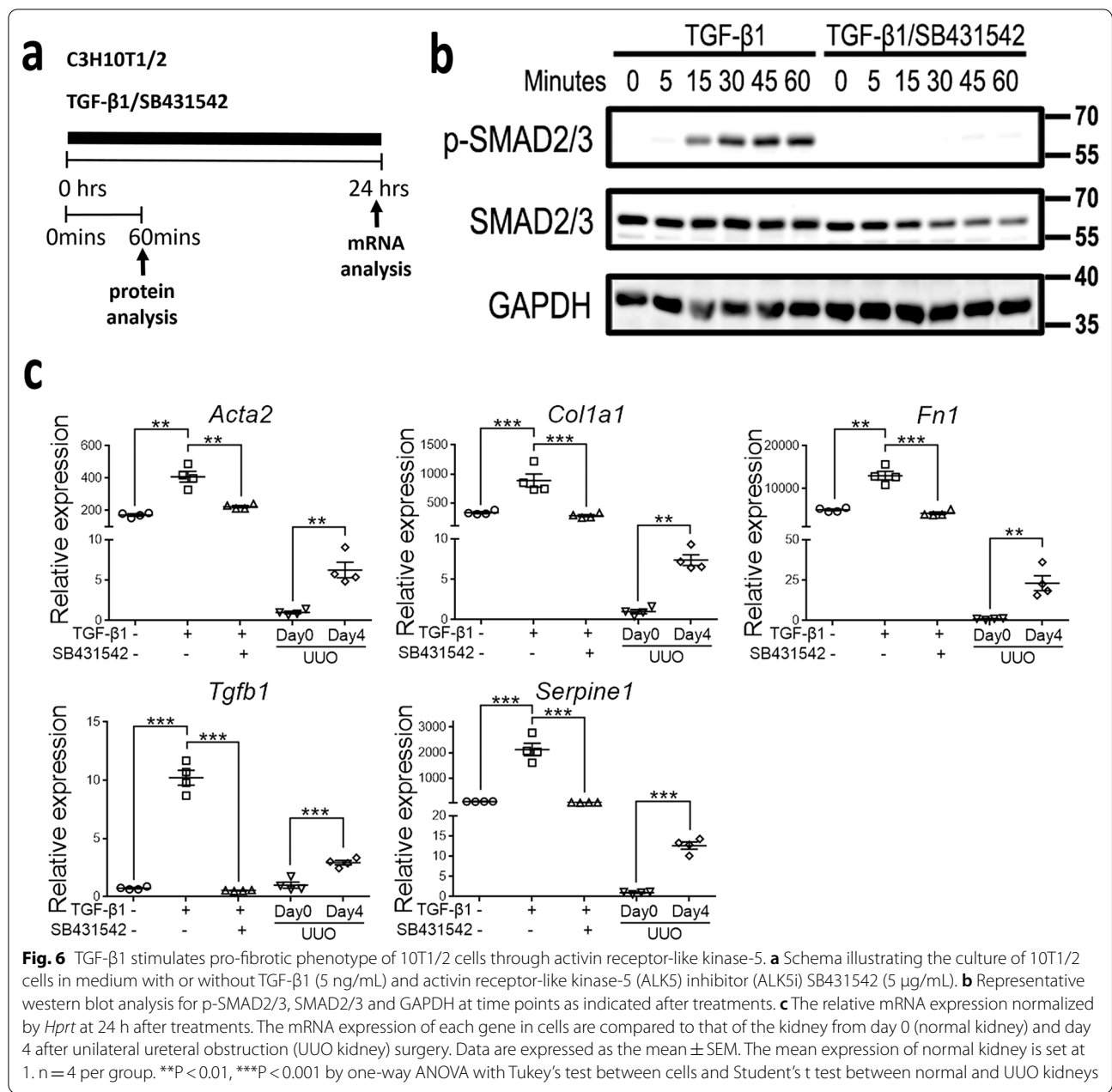
In contrast to our previous report on primary culture of kidney pericytes [3], TGF- $\beta$ 1 did not upregulate *Dnmt* genes which encoded DNMT in 10T1/2 cells even after 72-h exposure (Additional file 2: Fig. S7a, b). TGF- $\beta$ 1 did not change the methylation in 5'-flanking regions of *Epo* and *Epas1* genes (Additional file 2: Fig. S7c).

#### Pro-fibrotic kidney injury downregulated the expression of *Epas1* and *Epo* in pericytes

Our previous study has shown a prompt activation of TGF- $\beta$ 1-Smad2/3 signaling in kidney pericytes after pro-fibrotic injury induced by UO surgery [40]. Increased expression of *Tgfb1* and *Acta2* in the kidneys of WT mice after UO surgery was demonstrated again (Fig. 8a). In contrast, the expression of *Epas1* and *Epo* was decreased in the kidneys after UO surgery (Fig. 8a). In WT mice with ALK5i SB431542 treatment, the upregulation of *Acta2* while the downregulation of *Epas1* and *Epo* in the kidneys after UO surgery was reversed (Fig. 8b, c). We then used *Col1a1-GFP<sup>Tg</sup>* mice to isolate *Col1a1-GFP<sup>+</sup>* pericytes and myofibroblasts from the kidneys before and after UO surgery, respectively. Although the expression of *Acta2* was increased in myofibroblasts, the expression of *Hif1a*, *Epas1* and *Epo* was decreased in myofibroblasts (Fig. 8b, d). In *Col1a1-GFP<sup>Tg</sup>* mice with ALK5i SB431542 treatment, the expression of *Acta2* in myofibroblasts was decreased while the expression of *Hif1a*, *Epas1* and *Epo* was increased (Fig. 8b, e), a mechanism supporting the inhibitory effect of TGF- $\beta$ 1-ALK5 signaling on *Epas1-Epo* axis in REP pericytes.

#### Discussion

The main findings of this study included: (1) 10T1/2 cells represented a reliable cell line in the studies for EPO regulation and myofibroblast transition; (2) 10T1/2 cells expressed *Epo* through the binding of HIF2 $\alpha$  to 5'-enhancer and promoter of *Epo* gene; (3) TGF- $\beta$ 1 induced myofibroblast transition and repressed *Epas1-Epo* through ALK5 in 10T1/2 cells; and (4) pro-fibrotic injury activated TGF- $\beta$ 1-ALK5 signaling and repressed *Epas1-Epo* in REP pericytes in vivo, confirming the findings in 10T1/2 cells in vitro.



(See figure on next page.)

**Fig. 7** TGF-β1 inhibits HIF2α and *Epo* expression through ALK5 in 10T1/2 cells. **a** The relative *Epas1* expression normalized by *Hprt* in cells after exposure to TGF-β1 for the indicated duration. **b** Schema illustrating the analysis of HIFs in cells after 6-h exposure to normoxia or hypoxia in the presence or absence of TGF-β1. **c** Representative Western blot analysis for HIF1α, HIF2α and β-actin in cells of the experiment in **b**. Lower panels showing the expression of HIF1α and HIF2α which is normalized by β-actin. n = 3 per group. **d** Schema illustrating the analysis of HIFs in cells after 6-h exposure to normoxia or hypoxia in the presence or absence of TGF-β1 with or without ALK5i SB431542. **e** Representative Western blot analysis for HIF1α, HIF2α and α-tubulin in cells of the experiment in **d**. Lower panels showing the expression of HIF1α and HIF2α which is normalized by α-tubulin. n = 3 per group. **f** Schema illustrating the analysis of gene expression in cells after 24-h exposure to normoxia or hypoxia in the presence or absence of TGF-β1 with or without ALK5i SB431542. **g** The relative mRNA expression of *Epo*, *Hif1a* and *Epas1* normalized by *Hprt* in cells of the experiment in **f**. n = 4 per group. Data are expressed as the mean ± SEM. \*P < 0.05, \*\*P < 0.01, \*\*\*P < 0.001 by one-way ANOVA with Tukey's test

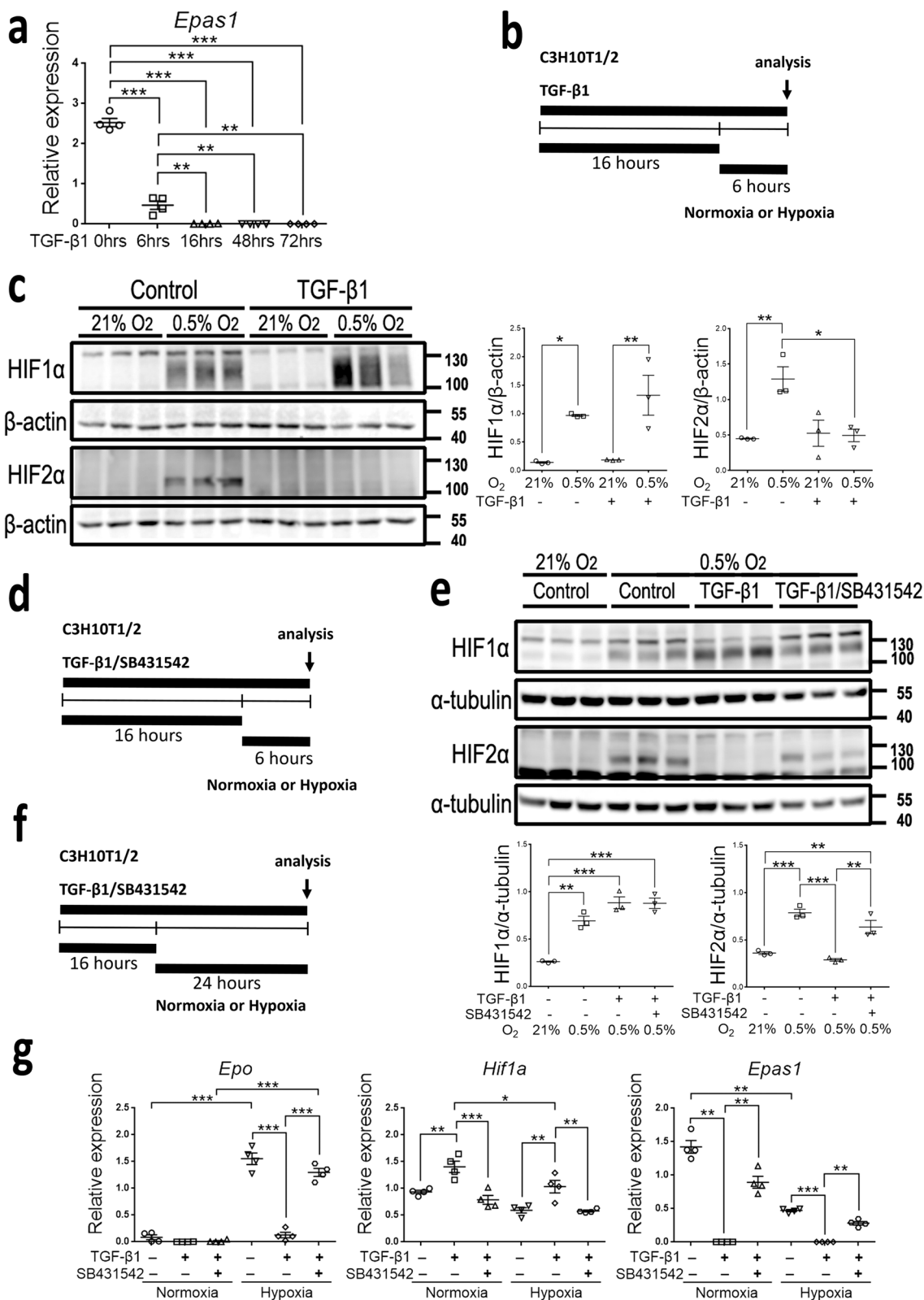


**Fig. 7** (See legend on previous page.)

10T1/2 cells did not express markers for epithelial cells, endothelial cells and podocytes. Similar to REP pericytes [3, 7, 9, 10, 12, 40], 10T1/2 cells expressed makers for mesenchymal cells. Compared to 3T3 cells, 10T1/2 cells expressed higher levels of *Pdgfrb*, *Ng2*, *Acta2*, *Col1a1*, *Col3a1* and  *which were expressed in REP pericytes [3, 7, 9, 10, 12, 40], suggesting 10T1/2 cells as a REP pericyte-like cell line. Previous studies have demonstrated that different subpopulations of kidney interstitial cells produce EPO and mostly are PDGFR $\beta^+$  [3, 4, 6, 19]. Interestingly, one of the reported REP cell lines, FAIK cells, exhibit telocyte-like phenotype [19]. 10T1/2 cells exhibited typical characteristics of fibroblasts. They did share features with telocytes including several prolongations and spindle shape of cell body. However, the main difference between 10T1/2 cells and telocytes was the cell processes. The processes of 10T1/2 cells were usually cone shape compared to those of telocytes which are moniliform aspect [41]. Besides, several studies indicate that renal telocytes are positive for CD34, CD117 and vimentin [42, 43]. We did not perform extensive transcriptomic analysis in 10T1/2 cells. However, it will be interesting to study whether 10T1/2 cells share telocyte-like gene expression profile in the future.*

In addition to produce EPO and myofibroblast transition that we demonstrated in this study, evidence has shown that 10T1/2 cells can stabilize microvasculature, an important property of pericytes [3, 8, 9, 37–39]. Compared to 3T3 cells which did not express *Epas1* and *Epo*, 10T1/2 cells showed substantially low methylation in 5'-flanking regions of *Epas1* and *Epo* genes, a finding supporting their capability as an EPO-producing cell line. Interestingly, HIF2 $\alpha$  expression was increased but *Epas1* expression was drastically decreased by hypoxia in 10T1/2 cells. Initially, we proposed a negative feedback leading to downregulation of *Epas1* when HIF2 $\alpha$  expression was increased by hypoxia. But we also found that hypoxia did not affect *Hif1a* expression even if HIF1 $\alpha$  was upregulated. A human cancer cell study has shown that *HIF1A* and *EPAS1* transcriptional response to hypoxia varies among human cells [44]. So far, we could not conclude the mechanism responsible for *Epas1* downregulation by hypoxia in 10T1/2 cells. Besides, we demonstrated that hypoxia could upregulate

*Slc2a1* expression in 3T3 cells, not in 10T1/2 cells. *Slc2a1* encodes solute carrier family 2 member 1 to enhance glucose transport in response to hypoxia [45]. The mechanism that 10T1/2 cells did not increase *Slc2a1* substantially in hypoxia needs further study.

Similar to REP pericytes, 10T1/2 cells expressed *Epo* through HIF2 $\alpha$ -activated transcription [3, 28]. Although 10T1/2 cells were not derived from the REP cells directly, our data demonstrated the major binding site for HIF2 $\alpha$  was the distal 5'-enhancer of *Epo* gene, a reported HRE located at KIE in the regulation of *Epo* expression [30]. FAIK cells and Replic cells are derived from the REP cells directly, but overexpression of SV40 large T antigen or human RAS results in hypermethylation and repression of *Epas1* and *Epo* genes [19, 20, 34, 35]. But similar to the findings in FAIK cells and Replic cells, 10T1/2 cells expressed extremely low level of *Epo* when compared to that of REP pericytes in normal kidneys. The mechanisms might be that 10T1/2 cells exhibited higher level of TGF- $\beta$ 1-ALK5 signaling and pro-fibrotic phenotype.

Sustained exposure to TGF- $\beta$ 1 has been shown to induce DNMT and hypermethylation of *Rasal1*, *Epo* and *Ybx2* in kidney pericytes [3, 9, 14]. In addition to the repressive effect of sustained TGF- $\beta$ 1 exposure through *Epo* hypermethylation [3], this study further demonstrated that short-term TGF- $\beta$ 1 exposure could downregulate *Epas1* and *Epo* of 10T1/2 cells in normoxia and hypoxia through an ALK5-dependent mechanism. In contrast to the inhibitory effect on the expression of *Epas1* and *Epo*, TGF- $\beta$ 1 increased the expression of *Hif1a*, *Egln1*, *Slc2a1* and *Vegfa* through ALK5 activation. *Egln1* upregulation might be involved in the downregulation of HIF2 $\alpha$  by increasing protein degradation. Notably, Souma et al. demonstrated disrupted hypoxic response in the kidney after UOU surgery, possibly due to over-activation of PHD in REP cells [15, 20]. Our previous data that TGF- $\beta$ 1 signaling increases soon after UOU-induced fibrotic injury and TGF- $\beta$ 1 represses *Epo* through hypermethylation after 72-h exposure [3, 40], and our finding in this study that TGF- $\beta$ 1 could repress *Epas1-Epo* within 24-h exposure suggested that TGF- $\beta$ 1 could inhibit EPO expression in REP cells via a dual mechanism—first via direct transcriptional repression and then via methylation. The dual mechanism by which TGF- $\beta$ 1 inhibits gene

(See figure on next page.)

**Fig. 8** Pro-fibrotic injury downregulates expression of *Epas1* and *Epo* of pericytes through ALK5. **a** The relative mRNA expression of *Tgfb1*, *Acta2*, *Hif1a*, *Epas1* and *Epo* in the kidneys at day 0 (normal kidney) and day 4 after UOU surgery (UOU kidney).  $n = 5$  at each time point. **b** Schema illustrating the analysis of kidneys and pericytes in mice with daily vehicle (Veh) or ALK5i SB431542 (5 mg/kg/day) treatment after UOU surgery. **c** The relative mRNA expression of *Acta2*, *Hif1a*, *Epas1* and *Epo* in the contralateral (CLK) and UOU kidneys of mice with daily Veh or ALK5i SB431542 treatment after UOU surgery according to the schema in **b**.  $n = 5$  at each time point. **d** The relative mRNA expression of *Acta2*, *Hif1a*, *Epas1* and *Epo* in Col1a1-GFP $^+$  pericytes isolated from kidneys before (day 0, normal kidney pericytes) and after (day 4 UOU kidney myofibroblasts) UOU surgery.  $n = 4$  at each time point. **e** The relative mRNA expression of *Acta2*, *Hif1a*, *Epas1* and *Epo* of Col1a1-GFP $^+$  myofibroblasts isolated from kidneys of mice with daily Veh or ALK5i SB431542 treatment at day 4 after UOU surgery according to the schema in **b**.  $n = 4$  per group. Data are expressed as the mean  $\pm$  SEM. \* $P < 0.05$ , \*\* $P < 0.01$ , \*\*\* $P < 0.001$  by Student's t test in **a**, **d** and **e**, and by one-way ANOVA with Tukey's test in **c**

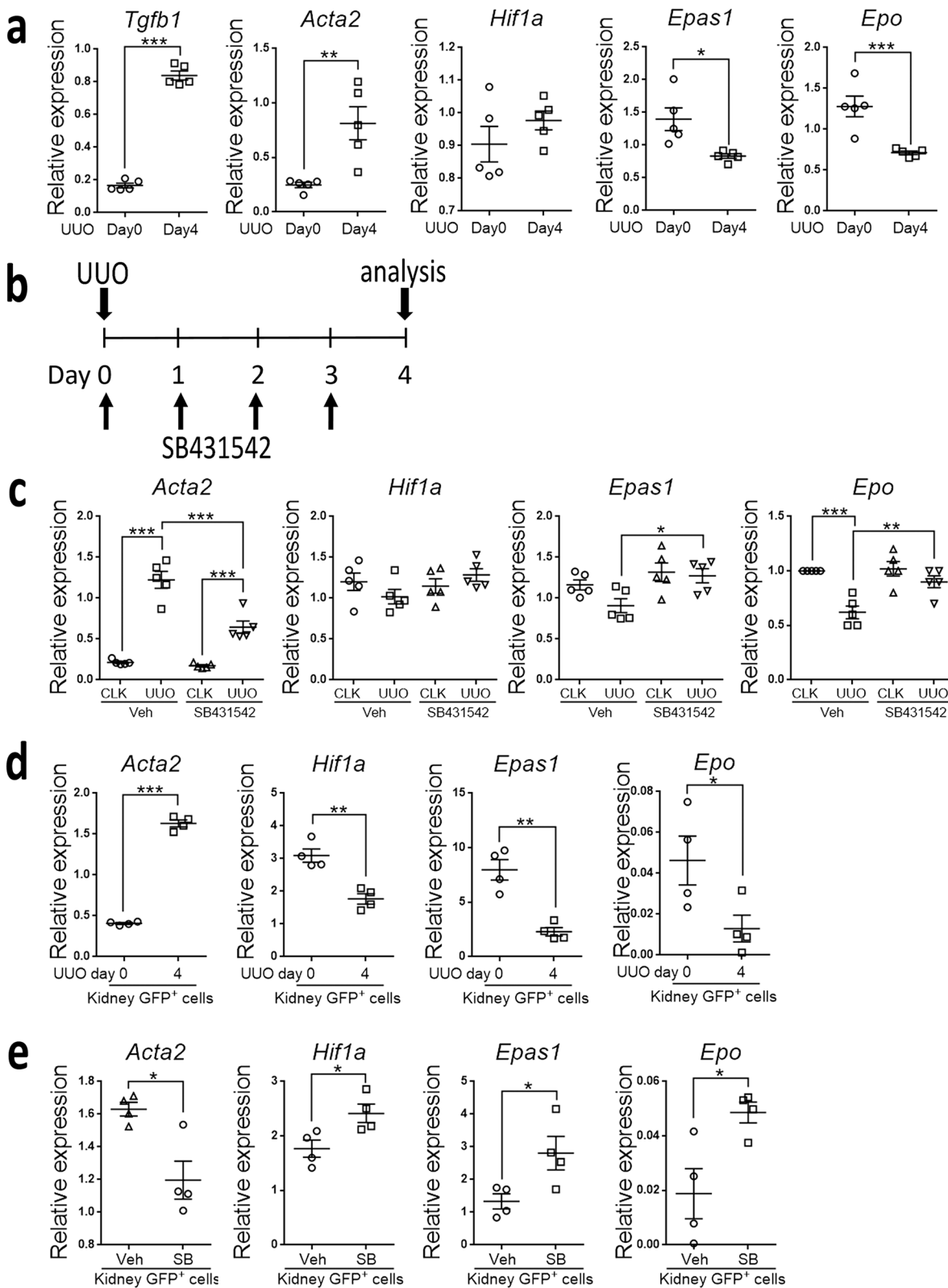


**Fig. 8** (See legend on previous page.)



expression seems common because TGF- $\beta$ 1 also inhibits *Rasal1* and *Ybx2* by the same mechanism [9, 14]. In the murine model of early renal fibrosis at day 4 after UUU surgery, we demonstrated that SB431542 could reverse *Epo* expression in the UUU kidney myofibroblasts through inhibiting TGF- $\beta$ 1-activated ALK5. Our finding could be supported by the recent report that selective disruption of TGF- $\beta$ 2 in renal PDGFR $\beta$ <sup>+</sup> cells preserves EPO production but no discernible effect on myofibroblast markers in the murine model of renal fibrosis [46].

In a personal communication with Norio Suzuki (Tohoku University), we knew that HIF2 $\alpha$  was not detected in interstitial cells of UUU fibrotic kidneys despite worsening hypoxia. This study demonstrated that PHDi could not increase HIF2 $\alpha$  expression of 10T1/2 cells in the presence of TGF- $\beta$ 1. However, PHDi emerges as a promising therapeutic agent for the renal anemia principally through stabilizing HIF [47–49]. One of the plausible reasons would be that a continuous spectrum existed between normal kidney pericytes and scar-producing myofibroblasts in fibrotic kidneys [3, 20]. In myofibroblasts with hypermethylation of *Epas1* and *Epo* genes, or with exposure to high TGF- $\beta$ 1, the effect of PHDi on HIF2 $\alpha$ -EPO expression would be limited. This proposal could be supported by the elegant study of Bernhardt et al. that PHDi FG-2216 fails to increase EPO in 2 of 6 hemodialysis patients with native kidneys in situ [50]. Chen et al. has also shown that a hemoglobin response (i.e., an increase of  $\geq 1.0$  g/dL from baseline) occurs in 85 of 101 CKD patients in the PHDi roxadustat group by week 9 after starting clinical trial, implying a poor response in 16% of patients [47]. Based on evidence from previous and current studies [3, 19, 20, 47, 50], the demethylating agent and ALK5i might provide additive therapeutic effect on EPO production.

In previous reports using Hep3B cells as the model, Faquin et al. demonstrate an inhibitory effect of TGF- $\beta$ 1 on hypoxia-induced EPO production [51], but Sánchez-Elsner et al. show the opposite result [52]. Hep3B cells, different from REP cells, produce EPO through binding HIF to liver specific 3'-enhancer [26, 29]. Sánchez-Elsner et al. demonstrate the interaction between TGF- $\beta$ 1-activated Smad3/4 and HIF1 $\alpha$  to enhance hypoxia-induced EPO production [52]. In contrast, we demonstrated the inhibitory effect of TGF- $\beta$ 1-ALK5 on *Epo* expression not only in 10T1/2 cells but also in murine fibrotic kidneys. To confirm the repressive effect of TGF- $\beta$ 1-ALK5 on kidney-specific *Epas1* or *Epo* regulation, we need to perform the reporter assay to study the repressive effect of Smad protein on the promoter/enhancer of *Epas1* and *Epo* genes in the future.

We did not find the hypermethylation of *Epas1* and *Epo* genes in 10T1/2 cells after 72-h exposure to TGF- $\beta$ 1, a

finding different from our previous report on primary culture of kidney pericytes [3]. The lack of increased DNMT by TGF- $\beta$ 1 in 10T1/2 cells might be one of the plausible reasons and provide a chance to serve a REP cell-like cell line for EPO biology study.

## Conclusions

Based on our data, the clonal mouse embryo cell line 10T1/2 expresses EPO through the major binding of HIF2 $\alpha$  to the 5'-HRE located at KIE of *Epo* gene. TGF- $\beta$ 1 not only promotes the transition of 10T1/2 cells to profibrotic phenotype but also represses *Epas1-Epo* expression. 10T1/2 cells serve a REP pericyte-like model for EPO biology study.

## Abbreviations

ALK5: Activin receptor-like kinase-5; ALK5i: ALK5 inhibitor; ANOVA: Analysis of variance;  $\alpha$ -SMA:  $\alpha$ -Smooth muscle actin; ChIP: Chromatin immunoprecipitation; DNMT: DNA methyltransferase; EPO: Erythropoietin; FAIK cell: Fibroblastoid atypical interstitial kidney cell; GFP: Green fluorescent protein; HIF: Hypoxia-inducible factor; HRE: Hypoxia response element; MSP: Methylation specific PCR; PDGFR: Platelet-derived growth factor receptor; PHD: Prolyl hydroxylase domain; PHDi: PHD inhibitor; REP cell: Renal EPO-producing cell; Replic cell: REP cell-derived immortalized and cultivable cell; SEM: Standard error of the mean; TGF- $\beta$ 1: Transforming growth factor- $\beta$ 1; UUU: Unilateral ureteral obstruction; VEGF-A: Vascular endothelial growth factor-A; 3T3 cell: NIH/3T3 cell; 10T1/2 cell: C3H10T1/2 cell.

## Supplementary Information

The online version contains supplementary material available at <https://doi.org/10.1186/s12929-021-00770-2>.

**Additional file 1. Table S1.** Primer sequences used in quantitative polymerase chain reaction. Table S2. Primer sequences used in (quantitative) chromatin immunoprecipitation polymerase chain reaction. Table S3. Primer sequences used in methylation-specific polymerase chain reaction of *Epo* and *Epas1* 5' flanking regions.

**Additional file 2. Figure S1.** Prolyl hydroxylase domain inhibitor induces hypoxia-inducible factor 1 $\alpha$  and hypoxia-inducible factor 2 $\alpha$  in C3H10T1/2 cells. Figure S2. siRNA transfection specific for *Hif1a* and *Epas1* downregulates hypoxia-induced genes. Figure S3. 10T1/2 cells exhibited higher levels of TGF- $\beta$ 1 signaling. Figure S4. TGF- $\beta$ 1 inhibits PHDi-induced HIF2 $\alpha$  expression through activin receptor-like kinase-5 in 10T1/2 cells. Figure S5. TGF- $\beta$ 1 inhibits hypoxia-induced nuclear accumulation of HIF2 $\alpha$  through ALK5 in 10T1/2 cells. Figure S6. TGF- $\beta$ 1 increases hypoxia-induced expression of *Egln1*, *Vegfa* and *Slc2a1* through ALK5 in 10T1/2 cells. Figure S7. TGF- $\beta$ 1 does not change methylation in 5' flanking regions of *Epo* and *Epas1* genes in 10T1/2 cells.

## Acknowledgements

The authors thank Dr. David Brenner (University of California, San Diego, CA) for *Col1a1-GFP*<sup>9</sup> mice, Chia-Chi Wu for technical assistance, the Department of Medical Research of National Taiwan University Hospital for equipment support, the Cell Sorting Core Facility of the First Core Laboratory, the Transgenic Mouse Model Core Facility of the National Core Facility Program for Biotechnology, Ministry of Science and Technology and the Gene Knockout Mouse Core Laboratory of the National Taiwan University Center of Genomic Medicine.

**Authors' contributions**

HMS, SYP, YHC, CYC, FCC, YTC and WCC carried out experiments and analyzed data. HMS, SYP, CJW, YHC, HCT and YMC participated in experiment design and data analysis. SLL designed and directed the project. HMS and SLL wrote the manuscript. All authors read and approved the final manuscript.

**Funding**

HMS is supported by Ministry of Science and Technology (Grant No. 110-2314-B-195-016) and MacKay Memorial Hospital (Grant No. MMH-110-33). SYP is supported by Ministry of Science and Technology (Grant No. 110-2314-B-002-292). SLL is supported by Ministry of Science and Technology (Grant No. 108-2314-B-002-078-MY3, 109-2314-B-002-260 and 110-2314-B-002-208), National Health Research Institutes (Grant No. EX108-10633SI), National Taiwan University Hospital (Grant No. 110-S4837 and 110-FTN05), National Taiwan University Hospital and National Taiwan University College of Medicine (Grant No. NSCCMOH-131-43), National Taiwan University (Grant No. NTU-CC-110L893304), Mrs. Hsiu-Chin Lee Kidney Research Foundation and Taiwan Health Foundation.

**Availability of data and materials**

All materials are available by the corresponding author.

**Declarations****Ethics approval and consent to participate**

All animal studies were conducted under a protocol approved by the Institutional Animal Care and Use Committee of the National Taiwan University College of Medicine (IACUC 20070217, 20210115).

**Consent for publication**

Not applicable.

**Competing interests**

The authors declare no competing interests.

**Author details**

<sup>1</sup>Graduate Institute of Physiology, College of Medicine, National Taiwan University, No. 1, Jen-Ai Road Section 1, Taipei 100, Taiwan. <sup>2</sup>Division of Nephrology, Department of Internal Medicine, Mackay Memorial Hospital, Taipei, Taiwan. <sup>3</sup>Department of Integrated Diagnostics and Therapeutics, National Taiwan University Hospital, Taipei, Taiwan. <sup>4</sup>Renal Division, Department of Internal Medicine, National Taiwan University Hospital, Taipei, Taiwan. <sup>5</sup>Division of Nephrology, Department of Internal Medicine, Far Eastern Memorial Hospital, New Taipei City, Taiwan. <sup>6</sup>Department of Medicine, Mackay Medical College, Taipei, Taiwan. <sup>7</sup>Department of Pharmacology, Graduate Institute of Medical Sciences, College of Medicine, Taipei Medical University, Taipei, Taiwan. <sup>8</sup>Department of Internal Medicine, National Taiwan University Hospital Jin-Shan Branch, New Taipei City, Taiwan. <sup>9</sup>School of Medicine, College of Medicine, National Taiwan University, Taipei, Taiwan. <sup>10</sup>Division of Chest Medicine, Department of Internal Medicine, National Taiwan University Hospital, Taipei, Taiwan. <sup>11</sup>Graduate Institute of Toxicology, College of Medicine, National Taiwan University, Taipei, Taiwan. <sup>12</sup>Research Center for Developmental Biology and Regenerative Medicine, National Taiwan University, Taipei, Taiwan.

Received: 2 August 2021 Accepted: 26 October 2021

Published online: 02 November 2021

**References**

- Asada N, Takase M, Nakamura J, Oguchi A, Asada M, Suzuki N, et al. Dysfunction of fibroblasts of extrarenal origin underlies renal fibrosis and renal anemia in mice. *J Clin Invest*. 2011;121(10):3981–90.
- Souma T, Yamazaki S, Moriguchi T, Suzuki N, Hirano I, Pan X, et al. Plasticity of renal erythropoietin-producing cells governs fibrosis. *J Am Soc Nephrol*. 2013;24(10):1599–616.
- Chang YT, Yang CC, Pan SY, Chou YH, Chang FC, Lai CF, et al. DNA methyltransferase inhibition restores erythropoietin production in fibrotic murine kidneys. *J Clin Invest*. 2016;126(2):721–31.
- Gerl K, Nolan KA, Karger C, Fuchs M, Wenger RH, Stolt CC, et al. Erythropoietin production by PDGFR-β(+) cells. *Pflugers Arch*. 2016;468(8):1479–87.
- Kobayashi H, Liu Q, Binns TC, Urrutia AA, Davidoff O, Kapitsinou PP, et al. Distinct subpopulations of FOXD1 stroma-derived cells regulate renal erythropoietin. *J Clin Invest*. 2016;126(5):1926–38.
- Broeker KAE, Fuchs MAA, Schrankl J, Kurt B, Nolan KA, Wenger RH, et al. Different subpopulations of kidney interstitial cells produce erythropoietin and factors supporting tissue oxygenation in response to hypoxia in vivo. *Kidney Int*. 2020;98(4):918–31.
- Lin SL, Chang FC, Schrimpf C, Chen YT, Wu CF, Wu VC, et al. Targeting endothelium-pericyte cross talk by inhibiting VEGF receptor signaling attenuates kidney microvascular rarefaction and fibrosis. *Am J Pathol*. 2011;178(2):911–23.
- Schrimpf C, Xin C, Campanholle G, Gill SE, Stallcup W, Lin SL, et al. Pericyte TIMP3 and ADAMTS1 modulate vascular stability after kidney injury. *J Am Soc Nephrol*. 2012;23(5):868–83.
- Chou YH, Pan SY, Shao YH, Shih HM, Wei SY, Lai CF, et al. Methylation in pericytes after acute injury promotes chronic kidney disease. *J Clin Invest*. 2020;130(9):4845–57.
- Lin SL, Kisseleva T, Brenner DA, Duffield JS. Pericytes and perivascular fibroblasts are the primary source of collagen-producing cells in obstructive fibrosis of the kidney. *Am J Pathol*. 2008;173(6):1617–27.
- Humphreys BD, Lin SL, Kobayashi A, Hudson TE, Nowlin BT, Bonventre JV, et al. Fate tracing reveals the pericyte and not epithelial origin of myofibroblasts in kidney fibrosis. *Am J Pathol*. 2010;176(1):85–97.
- Chen YT, Chang FC, Wu CF, Chou YH, Hsu HL, Chiang WC, et al. Platelet-derived growth factor receptor signaling activates pericyte-myofibroblast transition in obstructive and post-ischemic kidney fibrosis. *Kidney Int*. 2011;80(11):1170–81.
- Chang FC, Chou YH, Chen YT, Lin SL. Novel insights into pericyte-myofibroblast transition and therapeutic targets in renal fibrosis. *J Formos Med Assoc*. 2012;111(11):589–98.
- Bechtel W, McGoohan S, Zeisberg EM, Müller GA, Kalbacher H, Salant DJ, et al. Methylation determines fibroblast activation and fibrogenesis in the kidney. *Nat Med*. 2010;16(5):544–50.
- Souma T, Nezu M, Nakano D, Yamazaki S, Hirano I, Sekine H, et al. Erythropoietin synthesis in renal myofibroblasts is restored by activation of hypoxia signaling. *J Am Soc Nephrol*. 2016;27(2):428–38.
- Chiang CK, Tanaka T, Inagi R, Fujita T, Nangaku M. Indoxyl sulfate, a representative uremic toxin, suppresses erythropoietin production in a HIF-dependent manner. *Lab Invest*. 2011;91(11):1564–71.
- Chiang CK, Nangaku M, Tanaka T, Iwawaki T, Inagi R. Endoplasmic reticulum stress signal impairs erythropoietin production: a role for ATF4. *Am J Physiol Cell Physiol*. 2012;304(4):C342–53.
- Anusornvongchai T, Nangaku M, Jao T-M, Wu C-H, Ishimoto Y, Maekawa H, et al. Palmitate deranges erythropoietin production via transcription factor ATF4 activation of unfolded protein response. *Kidney Int*. 2018;94(3):536–50.
- Imeri F, Nolan KA, Bapst AM, Santambrogio S, Abreu-Rodríguez I, Spielmann P, et al. Generation of renal Epo-producing cell lines by conditional gene tagging reveals rapid HIF-2 driven Epo kinetics, cell autonomous feedback regulation, and a telocyte phenotype. *Kidney Int*. 2019;95(2):375–87.
- Sato K, Hirano I, Sekine H, Miyauchi K, Nakai T, Kato K, et al. An immortalized cell line derived from renal erythropoietin-producing (REP) cells demonstrates their potential to transform into myofibroblasts. *Sci Rep*. 2019;9(1):11254.
- Fried W. The liver as a source of extrarenal erythropoietin production. *Blood*. 1972;40(5):671–7.
- Yasuoka Y, Fukuyama T, Izumi Y, Nakayama Y, Inoue H, Yanagita K, et al. Erythropoietin production by the kidney and the liver in response to severe hypoxia evaluated by Western blotting with deglycosylation. *Physiol Rep*. 2020;8(12):e14485.
- Yamazaki S, Hirano I, Kato K, Yamamoto M, Suzuki N. Defining the functionally sufficient regulatory region and liver-specific roles of the erythropoietin gene by transgene complementation. *Life Sci*. 2021;269:119075.
- Goldberg MA, Glass GA, Cunningham JM, Bunn HF. The regulated expression of erythropoietin by two human hepatoma cell lines. *Proc Natl Acad Sci USA*. 1987;84(22):7972.

25. Yin H, Blanchard K. DNA methylation represses the expression of the human erythropoietin gene by two different mechanisms. *Blood*. 2000;95(1):111–9.
26. Ilaria MCO, Véronique NL, Federica S, Patrick S, Lisa C, Sara S, et al. Distal and proximal hypoxia response elements cooperate to regulate organ-specific erythropoietin gene expression. *Haematologica*. 2019;105(12):2774–84.
27. Rosenberger C, Mandriota S, Jürgensen JS, Wiesener MS, Hörstrup JH, Frei U, et al. Expression of hypoxia-inducible factor-1 $\alpha$  and -2 $\alpha$  in hypoxic and ischemic rat kidneys. *J Am Soc Nephrol*. 2002;13(7):1721.
28. Pan SY, Chiang WC, Chen YM. The journey from erythropoietin to 2019 Nobel Prize: Focus on hypoxia-inducible factors in the kidney. *J Formos Med Assoc*. 2021;120(1 Pt 1):60–7.
29. Suzuki N, Obara N, Pan X, Watanabe M, Jishage K-I, Minegishi N, et al. Specific contribution of the erythropoietin gene 3' enhancer to hepatic erythropoiesis after late embryonic stages. *Mol Cell Biol*. 2011;31(18):3896–905.
30. Storti F, Santambrogio S, Crowther LM, Otto T, Abreu-Rodríguez I, Kaufmann M, et al. A novel distal upstream hypoxia response element regulating oxygen-dependent erythropoietin gene expression. *Haematologica*. 2014;99(4):e45–8.
31. Plotkin MD, Goligorsky MS. Mesenchymal cells from adult kidney support angiogenesis and differentiate into multiple interstitial cell types including erythropoietin-producing fibroblasts. *Am J Physiol Renal Physiol*. 2006;291(4):F902–12.
32. Pan X, Suzuki N, Hirano I, Yamazaki S, Minegishi N, Yamamoto M. Isolation and characterization of renal erythropoietin-producing cells from genetically produced anemia mice. *PLoS ONE*. 2011;6(10):e25839.
33. Bussolati B, Lauritano C, Moggio A, Collino F, Mazzone M, Camussi G. Renal CD133+/CD73+ progenitors produce erythropoietin under hypoxia and prolyl hydroxylase inhibition. *J Am Soc Nephrol*. 2013;24(8):1234–41.
34. Lund P, Weisshaupt K, Mikeska T, Jammal D, Chen X, Kuban RJ, et al. Oncogenic HRAS suppresses clusterin expression through promoter hypermethylation. *Oncogene*. 2006;25(35):4890–903.
35. Tatenno M, Fukunishi Y, Komatsu S, Okazaki Y, Kawai J, Shibata K, et al. Identification of a novel member of the snail/Gli-1 repressor family, mlt 1, which is methylated and silenced in liver tumors of SV40 T antigen transgenic mice. *Cancer Res*. 2001;61(3):1144–53.
36. Reznikoff CA, Brankow DW, Heidelberger C. Establishment and characterization of a cloned line of C3H mouse embryo cells sensitive to postconfluence inhibition of division. *Cancer Res*. 1973;33(12):3231–8.
37. Darland DC, D'Amore PA. TGF $\beta$  is required for the formation of capillary-like structures in three-dimensional cocultures of 10T1/2 and endothelial cells. *Angiogenesis*. 2001;4(1):11–20.
38. Hara A, Kobayashi H, Asai N, Saito S, Higuchi T, Kato K, et al. Roles of the mesenchymal stromal/stem cell marker meflin in cardiac tissue repair and the development of diastolic dysfunction. *Circ Res*. 2019;125(4):414–30.
39. Zhou R, Liao J, Cai D, Tian Q, Huang E, Lü T, et al. Nupr1 mediates renal fibrosis via activating fibroblast and promoting epithelial-mesenchymal transition. *FASEB J*. 2021;35(3):e21381.
40. Wu CF, Chiang WC, Lai CF, Chang FC, Chen YT, Chou YH, et al. Transforming growth factor  $\beta$ -1 stimulates profibrotic epithelial signaling to activate pericyte-myofibroblast transition in obstructive kidney fibrosis. *Am J Pathol*. 2013;182(1):118–31.
41. Cretoiu SM, Popescu LM. Telocytes revisited. *Biomol Concepts*. 2014;5(5):353–69.
42. Li L, Lin M, Li L, Wang R, Zhang C, Qi G, et al. Renal telocytes contribute to the repair of ischemically injured renal tubules. *J Cell Mol Med*. 2014;18(6):1144–56.
43. Qi G, Lin M, Xu M, Manole CG, Wang X, Zhu T. Telocytes in the human kidney cortex. *J Cell Mol Med*. 2012;16(12):3116–22.
44. Chi JT, Wang Z, Nuyten DS, Rodriguez EH, Schaner ME, Salim A, et al. Gene expression programs in response to hypoxia: cell type specificity and prognostic significance in human cancers. *PLoS Med*. 2006;3(3):e47.
45. Abbud W, Habinowski S, Zhang JZ, Kendrew J, Elkairi FS, Kemp BE, et al. Stimulation of AMP-activated protein kinase (AMPK) is associated with enhancement of Glut1-mediated glucose transport. *Arch Biochem Biophys*. 2000;380(2):347–52.
46. Fuchs MAA, Broecker KAE, Schrankl J, Burzlaff N, Willam C, Wagner C, et al. Inhibition of transforming growth factor  $\beta$ 1 signaling in resident interstitial cells attenuates profibrotic gene expression and preserves erythropoietin production during experimental kidney fibrosis in mice. *Kidney Int*. 2021;100(1):122–37.
47. Chen N, Hao C, Peng X, Lin H, Yin A, Hao L, et al. Roxadustat for anemia in patients with kidney disease not receiving dialysis. *N Engl J Med*. 2019;381(11):1001–10.
48. Kurata Y, Tanaka T, Nangaku M. Hypoxia-inducible factor prolyl hydroxylase inhibitor in the treatment of anemia in chronic kidney disease. *Curr Opin Nephrol Hypertens*. 2020;29(4):414–22.
49. Pan SY, Tsai PZ, Chou YH, Chang YT, Chang FC, Chiu YL, et al. Kidney pericyte hypoxia-inducible factor regulates erythropoiesis but not kidney fibrosis. *Kidney Int*. 2021;99(6):1354–68.
50. Bernhardt WM, Wiesener MS, Scigalla P, Chou J, Schmieder RE, Günzler V, et al. Inhibition of prolyl hydroxylases increases erythropoietin production in ESRD. *J Am Soc Nephrol*. 2010;21(12):2151.
51. Faquin WC, Schneider TJ, Goldberg MA. Effect of inflammatory cytokines on hypoxia-induced erythropoietin production. *Blood*. 1992;79(8):1987–94.
52. Sánchez-Elsner T, Ramirez JR, Rodriguez-Sanz F, Varela E, Bernabéu C, Botella LM. A cross-talk between hypoxia and TGF- $\beta$  orchestrates erythropoietin gene regulation through SP1 and Smads. *J Mol Biol*. 2004;336(1):9–24.

## Publisher's Note

Springer Nature remains neutral with regard to jurisdictional claims in published maps and institutional affiliations.

Ready to submit your research? Choose BMC and benefit from:

- fast, convenient online submission
- thorough peer review by experienced researchers in your field
- rapid publication on acceptance
- support for research data, including large and complex data types
- gold Open Access which fosters wider collaboration and increased citations
- maximum visibility for your research: over 100M website views per year

At BMC, research is always in progress.

Learn more [biomedcentral.com/submissions](https://biomedcentral.com/submissions)

